ISSN 2176-5480

22nd International Congress of Mechanical Engineering (COBEM 2013)
November 3-7, 2013, Ribeirão Preto, SP, Brazil

A NUMERICAL ANALYSIS OF POWER COEFFICIENT BEHAVIOR FOR A HYDROKINETIC TURBINE MODEL

Bárbara Santana Rios
Allan Parente Vasconcelos
Lourenço Henrique Neves Guimarães
Luciano Gonçalves Noleto, lucianonoleto@unb.br
Universidade de Brasília, Faculdade UnB Gama, Área Especial de Indústria, Projeção A - UnB, Setor Leste - Gama - DF CEP: 72444-240

Abstract. *The objective of the present paper is to evaluate the power coefficient variation of a hydrokinetic turbine for some upstream conditions. Energy from river currents and channel flows can be used for power generation by hydrokinetic turbines. Inside this context, the turbine analyzed on the present paper aims to utilize the energy contained on the water that is not being used for power generation at the Tucuruí hydroelectric plant (Pará, Brazil). This paper approaches the study of the power coefficient of a geometry proposed for the turbine by CFD simulations. The conditions for the water flow of the river are known, and the other boundary conditions are determined according to the Fluid Dynamics classical theory. The ANSYS CFX commercial code is used to simulate the turbine. The simulations are performed varying the upstream river conditions. The obtained results showed a coherent behavior of the power coefficient.*

Keywords: *Hydrokinetic Turbines;Power Coefficient;Turbulence Modeling;Numerical Methods;Hydroelectric Plants*

1. INTRODUCTION

The Hydrokinetic turbine is a type of turbine that uses the stream energy from rivers and water courses directly. One of its advantages is the absence of dams, since the turbine is inside the river stream and anchored for energy production. The anchoring place is defined to obtain the best energy production. These turbines are defined as free flow turbines, just like wind turbines. Recent studies showed that using diffusers enhance the efficiency of the turbines, similarly to what draft tubes can do for reaction turbines (Filho (2001)).

Its utilization is motivated by the search of energetic solutions that brings low environment impact and to use locations that are not suited for construction of conventional hydroelectric power plants. Therefore, works on how to produce energy using hydrokinetic turbines on rivers (A. L. A. Mesquita and Cruz (1999) and A. L. A. Mesquita and Gouveia (2000)) or oceans (W.M.J. Batten and Chaplin (2008) and S.Bahaj and Meyers (2003)) were published at the recent decade.

Therefore, the present paper is inserted in a research project that aims to design a Hydrokinetic turbine to produce energy from water not used by conventional turbines at the Tucuruí Hydro plant. Its objective is to present results from a numerical simulation of the aforementioned turbine for different stream conditions. The ANSYS CFX commercial code is employed to perform the simulations. Results are showed in the form of velocity vectors, streamlines and power coefficient curves for each of the stream condition.

2. MATHEMATICAL MODELING

The mass conservation and momentum equations for incompressible flows are written in a framework of turbulence modeling and defined in an open connected bounded domain $\Omega_t \times [0,T]$ in $\mathbb{R}^d$ (where d=2 or 3) with boundary $\Gamma_t = \partial\Omega_t$ such as:

$$\nabla.\mathbf{u} = \mathbf{0} \tag{1}$$

$$\frac{\partial \mathbf{u}}{\partial t} + \mathbf{u}\cdot\nabla\mathbf{u} = -\frac{1}{\rho}\nabla p + \nabla(\nu + \nu_T)\nabla\mathbf{u} + f \tag{2}$$

In those equations $\mathbf{u}$ and p are the mean velocity and pressure fields, ν and ν_T are the kinematic and turbulent viscosity, respectively, ρ is the fluid density and f is the source term. One can note that the problem is open, since the turbulent viscosity needs modeling (Pope (2006)). The modeling approach is given by the SST turbulence model (Menter *et al.* (2003)):

$$\frac{\partial k}{\partial t} + \mathbf{u}\cdot\nabla k = P_k - \beta' k\omega + \nabla\cdot\left[\left(\nu + \frac{\nu_t}{\sigma_k}\right)\right]\nabla k \tag{3}$$

$$\frac{\partial \omega}{\partial t} + \mathbf{u}\cdot\nabla\omega \quad = \quad \alpha S^2 + \beta\omega + \nabla\cdot\left[\left(\nu + \frac{\nu_t}{\sigma_\omega}\right)\right]\nabla\omega$$

ISSN 2176-5480

$$+ \quad 2(1-F_1)\sigma_{\omega 2} + \frac{1}{\omega}(\nabla k)(\nabla \omega) \tag{4}$$

Here, k and ω are the turbulent kinetic energy and turbulent frequency respectively. The eddy viscosity is defined by:

$$\nu_t = \frac{\alpha_1 k}{\max(\alpha_1 \omega, SF_2)} \tag{5}$$

Here, S is an invariant measure of the rate-of-strain tensor and the blending functions F_1 and F_2 are given as follows:

$$F_1 = \tanh(\arg_1^4) \tag{6}$$

$$\arg_1 = \min\left[\max\left(\frac{\sqrt{k}}{\beta'\omega y}, \frac{500\nu}{y^2\omega}\right), \frac{4k}{CD_{k\omega}\sigma_{\omega 2} y^2}\right] \tag{7}$$

$$CD_{k\omega} = \max(2\frac{1}{\omega\sigma_{\omega 2}}\nabla k \nabla \omega, 1,0 \times 10^{-10}) \tag{8}$$

$$F_2 = \tanh(\arg_2^2) \tag{9}$$

$$\arg_2 = \max\left(\frac{2\sqrt{k}}{\beta'\omega y}, \frac{500\nu}{y^2\omega}\right) \tag{10}$$

Here, y is the distance to the nearest wall. The wall resolution for the simulations follows the guidelines of the SST turbulence model, where the dimensionless distance to the nearest wall y^+ should be below 2.

A production limiter is used to avoid the excessive generation of turbulence in stagnation points (Menter *et al.* (2003)):

$$P_k = \mu_t S^2 \tag{11}$$

$$\widetilde{P_k} = \min(P_k, 10 \cdot \rho\beta^* k\omega) \tag{12}$$

The constants of the model are accounted as a linear combination of the corresponding constants of the $k-\varepsilon$ and $k-\omega$ models (Menter *et al.* (2003)):

$$\alpha = \alpha_1 F_1 + \alpha_2(1-F_1) + ... \tag{13}$$

The constants are $\beta = 0.09$, $\alpha_1 = 5/9$, $\beta_1 = 3/40$, $\alpha_{k1} = 0.5$, $\sigma_{\omega 1} = 0.5$, $\alpha_2 = 0.44$, $\beta_2 = 0.0828$, $\sigma_{k2} = 1$, $\sigma_{\omega 2} = 0.856$. The ω-equation allows a near-wall formulation, which gradually switches from wall-functions to low-Reynolds near wall formulations (Menter *et al.* (2003)).

3. COMPUTATIONAL ASPECTS

The simulated domain and its mesh are displayed at figure 1:

ISSN 2176-5480

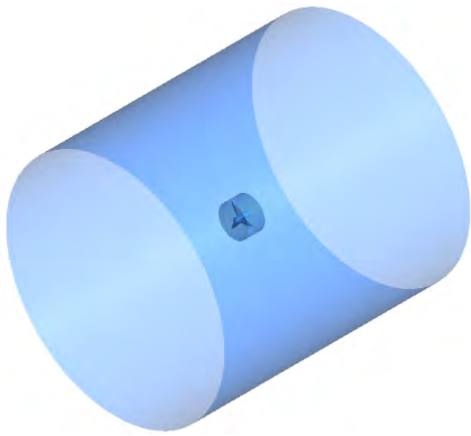

(a) Domain

(b) Mesh

Figure 1. Fluid Domain and Mesh

At the inlet, the velocities set for the inlet condition are 2.5 and 4 m/s . Under these flow velocities, the simulated rotation speed goes from 5 to 30 rpm. A zero reference pressure is imposed at the outlet boundary condition. At the turbine, a no-slip condition is imposed. The mesh statistics are: 940029 nodes e 4165416 elements. The power coefficient is calculated as follows:

$$C_p = \frac{P}{0.5\rho U_0^3 A} \tag{14}$$

Where P is the power input, ρ is the fluid density, A is the span area of the turbine and U_0 is the stream flow velocity.

4. RESULTS AND DISCUSSIONS

Figure 2 shows the streamline visualization of the flow downstream to the turbine. Its colors show the velocity variation at that direction. One can note that the flow shows the longitudinal vorticity expected from the turbine movement and its spinning effect on the flow. Also, the same vorticity is observed at the core of the turbine. This vorticity is not expanded or reduced in the downstream. There is no secondary flow at the turbine, indicating the absence of energy loss due to turbulence. Since this turbine operates as a free-flow turbine, its power coefficient cannot be above 0.59 to obey Betz' principle.

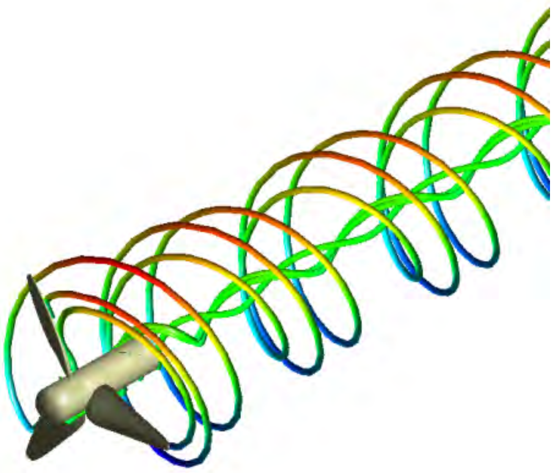

Figure 2. Streamlines at Downstream

Figure 3 shows the surface streamlines plotted at the turbine surface in front and back views. One can note stagnation points at the tips of the blades due to the change of the flow direction. But there are no stagnation regions at the surface of the blades. Those streamlines shows the normal rotation movement at the turbine region. There are also no signs of secondary flow nor detached flow in both surfaces. One can conclude that the hydrodynamic behavior at the surroundings of the turbine is adequate, without energy flow loss.

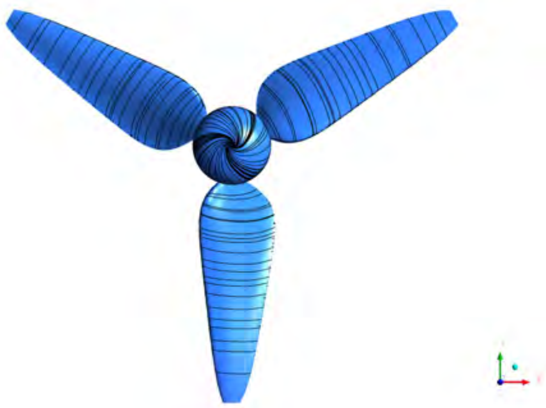

(a) Front

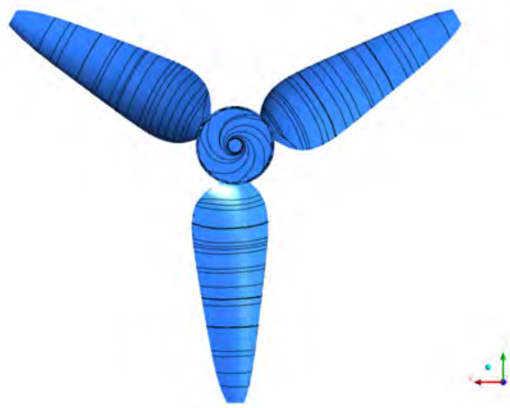

(b) Back

Figure 3. Surface Streamlines

Figure 4 shows the pressure field at the surface of the turbine in front and back views. High pressure zones are observed at the front view (red zones), followed by low pressure regions (blue zones). This effect is coherent with what is expected for this kind of flow. At the back view, one can observe low pressure zones, due to flow passage and the rotation effect. These effects are also credited to the correct hydrodynamic project of the blades. The blades has the correct angulation, avoiding adverse effects such as secondary flows and undesired vortices. Those effects cause low pressure zones that can lead to problems with cavitation.

Figure 5 shows the power coefficient variation for several values of the tip speed ratio λ. All velocities show the typical C_p behavior for free-flow turbines, where in a certain value of λ, the coefficient has its maximum value, and then decreases. After that decrease, the coefficient increase again, for high values of tip speed ratio. It is important to highlight that all velocities respect the Betz principle, where the maximum power coefficient should not surpass the value of 0.59. For the flow velocity of 1.5 m/s, the first peak of C_p occurs at a $\lambda = 2.30$. Afterwards, its value increases close to the Betz limit to a high tip speed ratio. One can consider that this result represent a point where the turbine should not be operating, since the rotation is too high. The velocities of 2 and 2.5 m/s shows similar behaviors, differentiated by the value of λ where the peak occurs. Also, those two velocities showed the increase of C_p after the peak. The flow velocity of 4 m/s shows a similar value of the coefficient at its peak. One can conclude that the maximum C_p for all velocities is between 0.37 and 0.39. Therefore, for this blade configuration, one can conclude that the optimum condition for this turbine is the rotation of 20 rpm (λ=4.6) and the velocity of 2.5 m/s.

ISSN 2176-5480

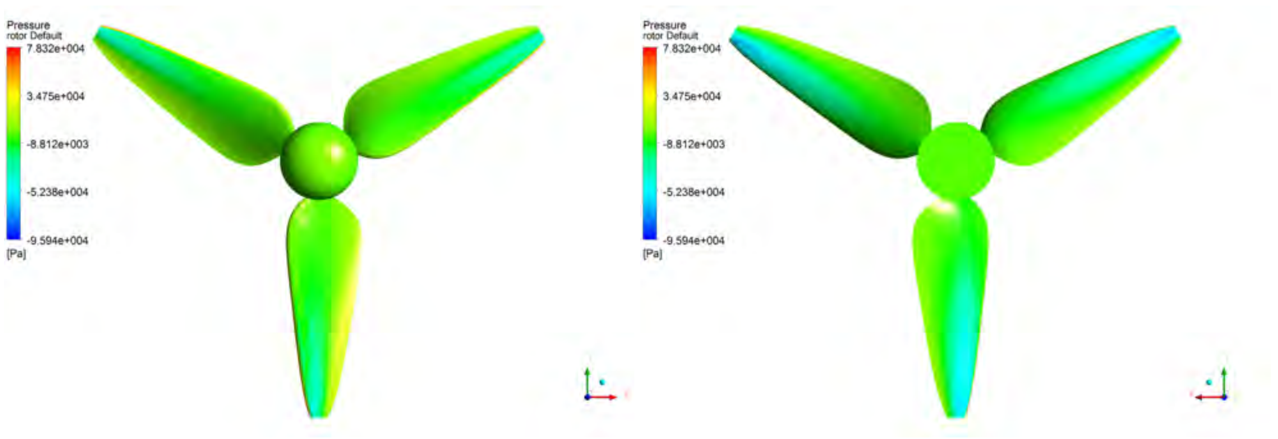

(a) Front (b) Back

Figure 4. Pressure at the Turbine Surface

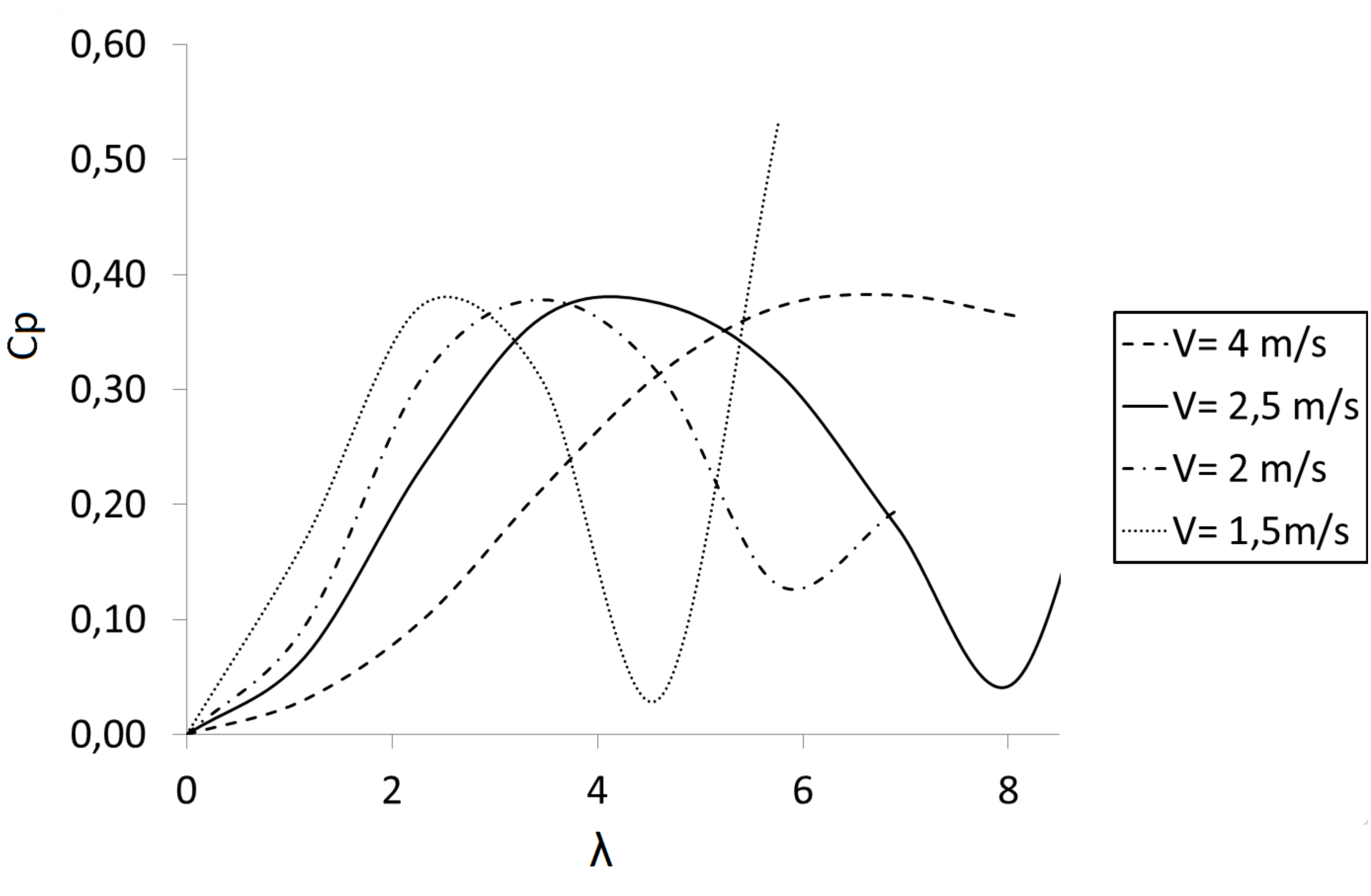

Figure 5. Power Coefficient

5. CONCLUSIONS

Results of the numerical simulation of the flow over a hydrokinetic turbine were showed for two free flow velocities. The flow at the surroundings of the turbine is evaluated to characterize the turbine operation. It is observed that the flow presents a typical longitudinal vorticity, due to the rotation movement of the turbine. There is no secondary flows at the turbine, indicating no energy flow loss. The turbine hydrodynamic project and assembly are adequate, and this characteristic is confirmed by the absence of secondary or detached flows at the blade. The power coefficient results showed coherent results, that respected Betz' principle. The condition that provided the maximum value of C_p is the rotation of 20 rpm and velocity of 2.5 m/s.

Therefore, one can conclude that the results were able to characterize the turbine optimum configuration. Future

ISSN 2176-5480

research steps for this turbine are:

- Simulation of the turbine with diffusers, in order to increase the power coefficient;
- Simulation of the turbine with different flow conditions, in order the make a complete characterization of the flow configuration of the turbine.

6. ACKNOWLEDGEMENTS

The authors wish to thank ELETRONORTE for the financial support, under the TUCUNARÉ project.

7. REFERENCES

A. L. A. Mesquita, C.J.B. and Gouveia, M.S., 2000. "Analisis hidrodinamica de rotores axiales para uso de energia cinetica de los rios". *Revista Informacion Tecnologica del Chile*, Vol. 21.

A. L. A. Mesquita, C.M.V.S. and Cruz, D.O.A., 1999. "A simplified method for axial flow turbomachinery design". *Journal of the Brazilian Society of Mechanical Sciences and Engineering*, , No. 21, pp. 61–70.

Filho, G.L.T., 2001. "The state of art of hydrokinetic power in brazil". In *Anais da Waterpower XIII Conference, Buffalo-New York, USA*.

Menter, F.R., Kuntz, M. and Langtry, R., 2003. "Ten years of industrial experience with the sst turbulence model". *Turbulence, Heat and Mass Transfer*, Vol. 4.

Pope, S.B., 2006. *Turbulent Flows*. Cambridge University Press.

S.Bahaj, A. and Meyers, L.E., 2003. "Fundamentals applicable to the utilization of marine current turbines for energy production". *Renewable Energy*, , No. 28, pp. 2205–2211.

W.M.J. Batten, A.S. Bahaj, A.M. and Chaplin, J., 2008. "The prediction of the hydrodynamic performance of marine current turbines". *Renewable Energy*, , No. 33, pp. 1085–1096.

8. RESPONSIBILITY NOTICE

The authors are the only responsible for the printed material included in this paper.